Electronic Supplementary Material (ESI) for Nanoscale
This journal is © The Royal Society of Chemistry 2012

Supplementary Information

One-Dimensional Ferromagnetic Dendritic Iron Wire Array Growth by Facile Electrochemical Deposition

Ri Qiu,[a] Jin You Zheng,[b] Hyun Gil Cha,[b] Myung Hwa Jung,[c] Kyu Joon Lee,[c] and Young Soo Kang [b]*

[a] *Institute of Oceanology, Chinese Academy of Sciences, 7 Nanhai Road, Qingdao 266071, China.*

[b] *Department of Chemistry, Sogang University, Seoul, South Korea.*

Fax: (+82)-2-701-0967; E-mail: yskang@sogang.ac.kr.

[c] *Department of Physics, Sogang University, Seoul, South Korea.*

This journal is © The Royal Society of Chemistry 2012

SI 1. Experimental details and characterization

Preparation of dendritic Fe.

Characterization of dendritic Fe structure.

One dimensional dendritic iron array wettability measurement.

Preparation of dendritic Fe_2O_3.

SI 2. The effect of deposition conditions

SI 3. The superhydrophilicity wettability of one dimensional dendritic iron array

SI 4. Fig. S1-Fig. S5

This journal is © The Royal Society of Chemistry 2012

S1. Experimental details and characterization

Preparation of dendritic Fe. The preparation of iron material was performed in a simple three-electrode cell by using an EG&G potentiostat/galvanostat M263 A instrument. High-purity Cu foil (Aldrich, 99.98%), which was scratched by sandpaper and cleaned with deionized water (>18 MΩ·cm, Nanopure Ultrapure water system), was used as the substrate for iron electrochemical growth. A coiled Pt wire electrode was applied as the counter electrode, and a saturated calomel electrode (SCE) was the reference electrode. Unless indicated specifically, all the potentials reported in this study were quoted with SCE as the reference electrode. The distance between working and counter electrodes was ~ 2.0 cm. The tip of the reference electrode was in the vicinity of the working electrode. Mixed solution containing 0.05 M $FeSO_4$ (Aldrich) and 0.1 M Na_2SO_4 (Shinyo Pure Chemicals, G. R. reagent) was added into the cell as the precursor solution for iron crystal growth. The pH of the solution was adjusted with H_2SO_4.

The chronoamperometry technique was applied for the electrochemical growth of iron from the solution. The electrochemical process was performed in a stationary electrolyte solution without any stirring or protective gas bubbling. After electrolysis, the electrode was seceded from the solution and washed several times with deionized water and acetone to remove impurities. For the further characterization, the materials were dried promptly and stored in the cyclohexane to avoid oxidation.

Characterization of dendritic Fe structure. The morphology of the material was characterized by field-emission scanning electron microscopy (FE-SEM, JEOL, JSM-6700F) and high-resolution transmission electron microscope (HRTEM, JEOL. JEM-2100F). Selected area electron diffraction (SAED, JEOL. JEM-2100F, 200.0 KV) was used to reveal the crystal structure. Energy-dispersive spectroscopy (EDS, Oxford Instruments, INCA x-sight) was applied to analyze the elemental composition in the obtained material. X-ray diffraction (XRD, Rigaku, MiniFlex II desktop X-ray diffractometer. The X-ray is Cu Kα radiation with λ = 0.154056 nm.) was used to verify the material phase deposited on the copper substrate. Magnetic property measurement system superconductor quantum interference device vibrating sample magnetometer (MPMS SQUID-VSM) was used to measure the magnetic property of the deposit in magnetic field ranging from -70 000 to +70 000 Oe at room temperature.

Preparation of dendritic Fe_2O_3.

The as-prepared dendritic Fe wire array films were annealed in air at 500 ^oC for 2 h using an AJEON box furnace. The films were heated and cooled at a rate of approximately 2 ^oC/min.

One dimensional dendritic iron array wettability measurement.

The as-grown one dimensional dendritic iron array was dried in the N_2 flow to make sure no water

remaining. A Phoenix 300 contact angle measurement instrument was used for the wettability measurement. The water droplet was shot to the array surface by a microliter scale syringe.

SI 2. The effect of electrodeposition conditions

During the electrolysis of mixed solution containing $FeSO_4$ and Na_2SO_4, applied potential and solution pH are the key parameters to determine the final products. Maintaining a constant concentration of $FeSO_4$ and Na_2SO_4, multiple experiments with different potential and pH were conducted to illustrate their impacts to the deposits. During the electrolysis, there are two reactions existing on the working electrode surface, i.e., $2H^+ + 2e = H_2$ (1) and $Fe^{2+} + 2e = Fe$ (2), which makes the process complicated. Depending on the condition, any one can be the dominant one. The dependence relationship among potential, pH and final products are critical for the deep understanding of the system and the one dimensional iron material formation mechanism. Herein, based on the primary results, one concise *product map* (Fig. S1a) is demonstrated to illustrate the relationship between the electrolysis conditions and the products.

For the applied potential, it affords the motivation for the electrodeposition. With the less negative potential (e. g., -1.00 V) located in region I, the drive force is below the critical potential[1-3] for dendritic structure formation and it can only enable the electroplating. Electrode 2 in Fig. S1b with smooth and shiny surface is obtained in this region. When the potential adopts more negative values to reach region II and IV, i. e., surpassing the critical potential, there will be the dendritic structure formed. Compared to the electroplating appearance, the deposit on the substrate is black (electrode 3 in Fig. S1b), which is due to the low light reflectance of the dendritic structure. If the applied potential reaches region III, the more negative potential will favor the reaction $2H^+ + 2e = H_2$. There is severe bubbling generated on the electrode, and precipitate is formed in the solution. The generation of large amount of H_2 will consume H^+ and further drive the reaction $H_2O = H^+ + OH^-$ to produce more OH^-, which will steadily react with Fe^{2+} to form the precipitate.

For pH parameter, if the solution pH is high, there will be precipitate formed in the solution due to the reaction between Fe^{2+} and OH^-. On the contrary, if the pH is too low, the H^+ will be plentiful enough to compete with Fe^{2+} to be reduced on the cathode (region V). The H_2 evolution will be the main reaction instead of the iron deposition.

From our experimental results, we find that the 1-D iron wire structure can only be obtained in region IV with appropriate pH and potential values. In a typical experiment, when the pH of the solution was decreased to 2.47, the one dimensional structure will be obtained by the electrolysis. For the higher pH value electrolysis, the ordinary dendrites lying on the substrate will be obtained. Up to now, the reason is

still ambiguous to us. The research is still being carried on in our lab now.

SI 3. The superhydrophilicity wettability of one dimensional dendritic iron array

When contact angle between solid and water phase is less than 5^o, superhydrophilicity is realized. This phenomenon has great opportunity for application in different fields such as antifogging, antifreezing and thermal engineering fields.[4-6] As shown in Fig. 5b, the one dimensional channels are irregularly surrounded by the dendrites, but they have short width. As approximation, the channels are taken as round with the diameter of ca. 1 μm. According to the well-known Young-Laplace equation, $p = 2\gamma/R$, in which p, γ and R respectively represent the additional pressure, water surface tension and radius of curvature, the capillary force p is calculated as $p = 2\times0.07214/(0.5\times10^{-6}) = 2.89\times10^5$ Pa. When water droplet is in contact with the surface of one dimensional dendritic iron wire array, the pressure can certainly drive the water to go into the channels of array. Moreover, since channels are interconnected each other, the air will escape from channels by the incoming water drive. When water enters into the channel, the smaller channels between branches will exert the relay capillary force to drive water to spread further. As shown in Fig. 3a, channels formed among branches are ca. 50 nm. The capillary force p is approximated as $p = 2\times0.07214/(25\times10^{-9}) = 5.77\times10^6$ Pa (nearly 57 atm). Under such a strong force, the water droplet will spread rapidly along the dendrite veins, which leads to superhydrophilicity wettability. As shown in Fig. S4, when 2 μL water droplet is in contact with the array, the water spreads so rapidly that no water is remaining to be observed. With another 2 μL water droplet, the surface reveals the typical superhydrophilicity with the contact angle below 5^o. Since the dendritic Fe wire array is formed on copper substrate, this super hydrophilic phenomenon suggests a potential application in the thermal engineering field.

SI 4. Fig. S1-Fig. S5

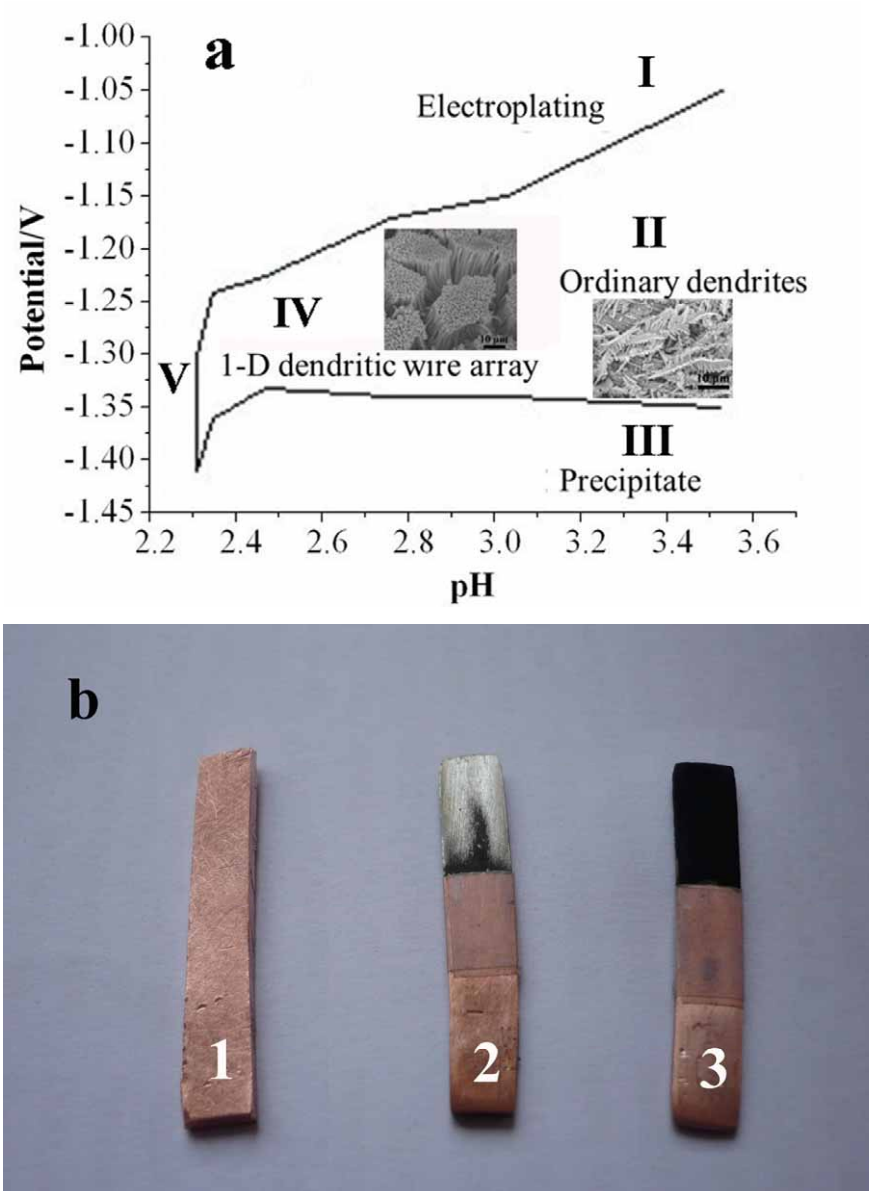

Fig. S1. (a) The *product map* of the electrolysis products of the aqueous $FeSO_4$ solution. Both the bars shown in the two SEM images represent 10 μm. (b) The photograph image of different electrodes. Electrode 1 is a naked copper substrate; electrodes 2 and 3 are obtained by electrodeposition from the region I and IV, respectively.

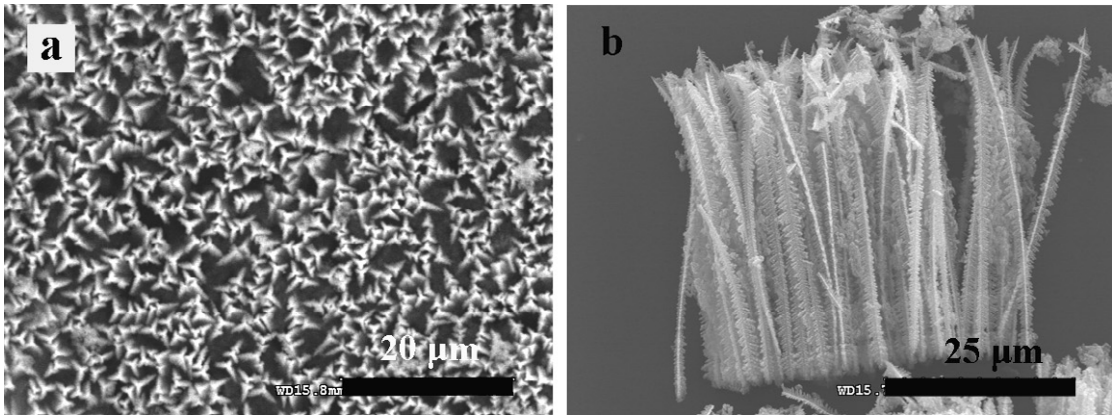

Fig. S2. As-grown one-dimensional Fe dendritic wires show homogeneous length.

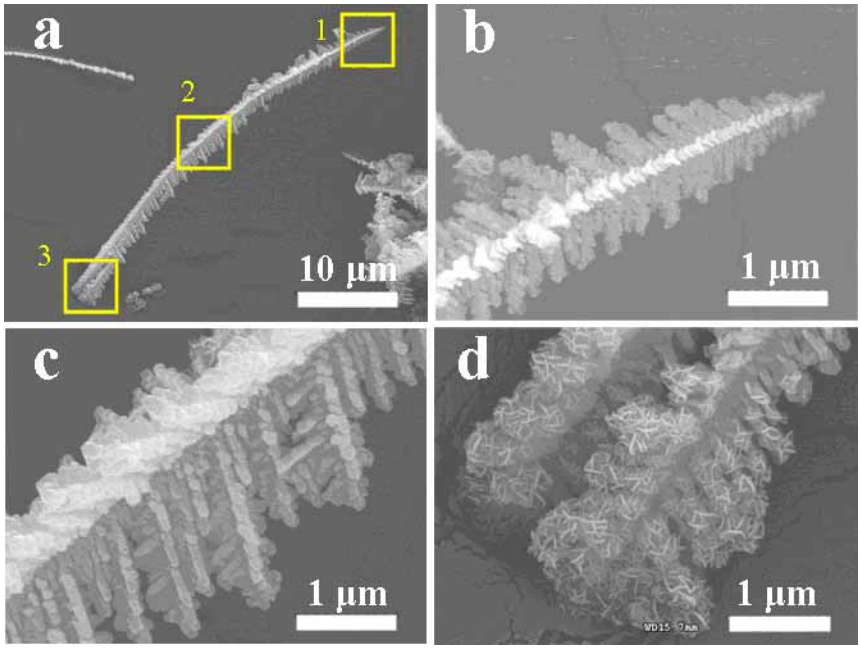

Fig. S3. High resolution SEM of one-dimensional Fe dendritic wire.

This journal is © The Royal Society of Chemistry 2012

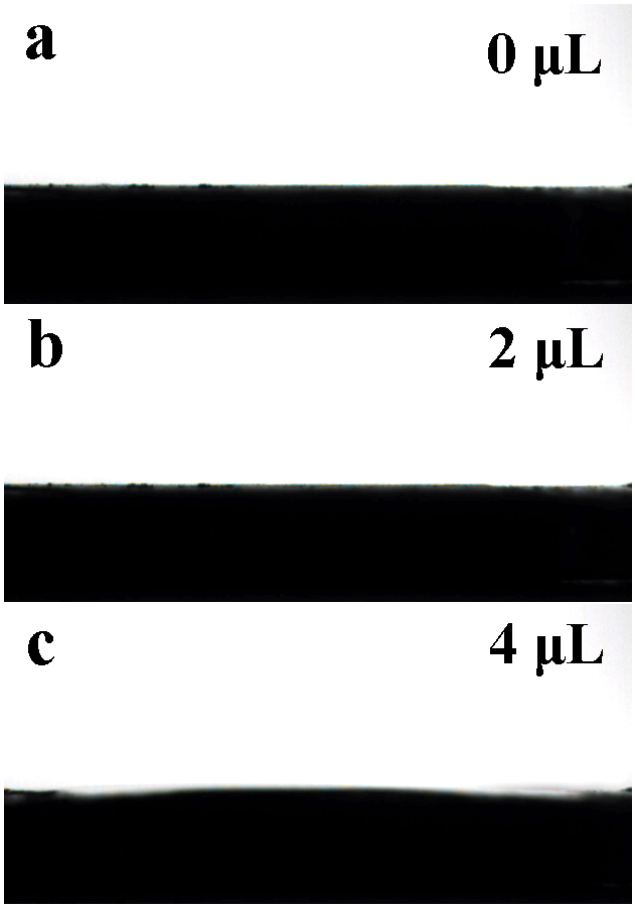

Fig. S4. The wetting scenario of various amount of water on the surface of the one-dimensional iron dendritic wire array. (a) the initial state; (b) after injection of 2 μL water; (c) after injection of 4 μL water.

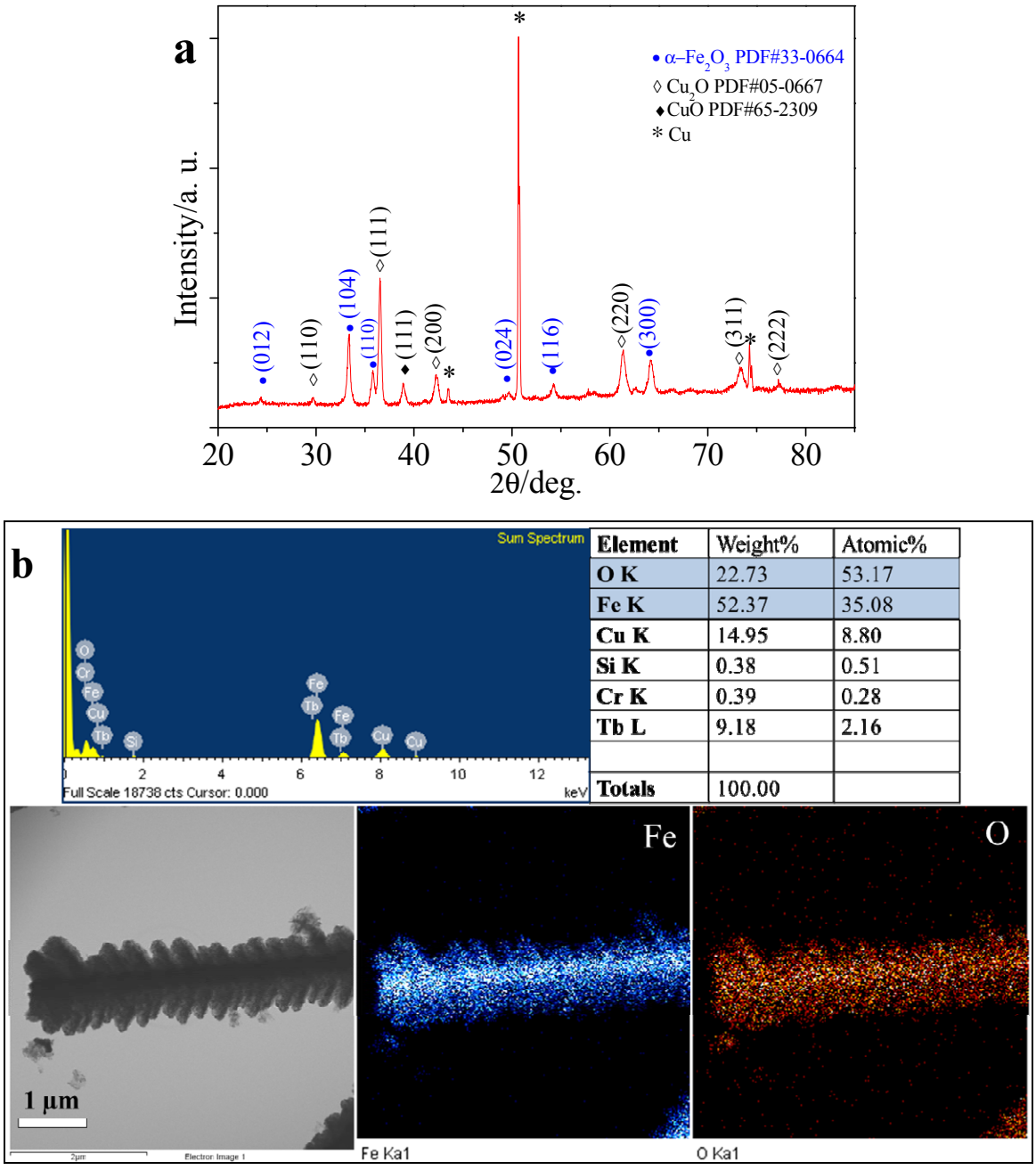

Fig. S5. (a) XRD, (b) EDS and EDS-mapping of Fe films on Cu Substrate after annealing 500 ^{o}C for 2 h. EDS spectrum processing: No peaks omitted and all elements analyzed. Cu, Si, Cr and Tb come from Cu grid.

This journal is © The Royal Society of Chemistry 2012

Reference

1 K. I. Popov, Lj. M. Djukić, M. G. Pavlović and M. D. Maksimović, *J. Appl. Electrochem*., 1979, 9, 527-531.

2 K. I. Popov, M. G. Pavlović, M. D. Spasojević and V. M. Nakić, *J. Appl. Electrochem*., 1979, 9, 533-536.

3 N. D. Nikolić, K. I. Popov, L. J. Pavlović and M. G. Pavlović, *Sensors*, 2007, 7, 1-15.

4 A. Asatekin, S. Kang, M. Elimelech and A. M. Mayes, *J. Memb. Sci*., 2007, 298, 136-146.

5 M. Nie, P. Patel, S. Kai and D. D. Meng, In Superhydrophilic Anti-Fog Polyester Film by Oxygen Plasma Treatment, Proceedings of the Nano/Micro Engineered and Molecular Systems, January 2009, Shenzhen, China. NEMS 2009. 4th IEEE International Conference, 1017-1020.

6 Y. Takata, S. Hidaka, M. Masuda and T. Ito, *surface. Int. J. Energ. Res*., 2003, 27, 111-119.